Supporting Information

5-[(Pyren-9-ylmethyl)amino]isophthalic Acid with Nitrogen Containing Heterocylces: Stacking, N-H···π Interactions and Photoluminescence

Jagajiban Sendh, Munendra Pal Singh, Jubaraj B. Baruah

List of Figures and Tables

Captions of Figures and Tables

Spectroscopic data for the cocrystals:

H_2L·DMF: Isolated yield: 62 %. ^{1}HNMR (600 MHz, DMSO, ppm): 12.97 (2H, s), 8.46 (1H, d, *J* = 9.2 Hz), 8.29 (5 H, m), 8.16 (1H, s), 8.09 (2H, dt, *J* = 7.5, 3.6Hz), 7.95 (1H, s from C-H of DMF), 7.70 (1H, s), 7.47 (2H, s), 7.06 (1H, t, *J* =5.5 Hz), 5.07 (2H, d, *J* = 5.4 Hz) 2.86 (s, N-Me), 2.76 (s N-Me). IR (KBr): 3502 (m), 3425 (s), 3124 (m), 1668 (s), 1601 (s), 1515 (s), 1424 (m), 1316 (m), 1262 (m), 1216 (s), 1089 (m), 924 (m), 837 (s), 810 (s), 755 (s), 708 (m), 667 (s), 539 (m), 486 (m). UV-vis (solid, λ_{max}, nm) 400 nm. 1HNMR of crude sample of **H_2L** without DMF: ^{1}HNMR (600 MHz, DMSO, ppm) :12.97 (2H, bs), 8.46 (1H, d, *J* = 9.2 Hz), 8.29 (5H, m), 8.16 (1H, s), 8.11 – 8.07 (2H, m), 7.71 (1 H, s), 7.47 (2H, s), 7.05 (1H, t, *J* = 5.3 Hz), 5.07 (2H, d, *J* = 5.3 Hz).

H_2L·DMPA Isolated yield: 66 %. ^{1}HNMR (600 MHz, DMSO, ppm) :12.89 (2H, s), 8.47 (1H, d, *J* = 9.2 Hz), 8.38 – 8.21 (5H, m), 8.16 (1H, s), 8.09 (2H, t, *J* = 7.2 Hz), 7.71 (1H, s), 7.48 (2H, s), 7.02 (1H, s), 6.33 (2H, d, *J* = 10.2 Hz), 5.07 (2H, d, *J* =5.1 Hz), 2.16 (6H, s). IR (KBr, cm^{-1}) 3506 (w), 3401 (w), 3294 (w), 3178 (m), 1883 (br,w), 1688(s), 1664 (s), 1599 (s), 1507 (w), 1459 (m), 1365 (s), 1269 (s), 851(s), 756 (s). UV-vis (solid, λ_{max}) 397 nm.

H_2L·Caffeine·3H_2O: Isolated yield of crystals: 15 %. ^{1}HNMR (600 MHz, DMSO, ppm): 12.97 (2H, s), 8.47 (1H, d, *J* = 9.2), 8.30 (5H, m), 8.16 (1H, d, *J* = 1.6 Hz), 8.12 – 8.07 (2H, m), 8.01 (1H, s), 7.70 (1H, s), 7.47 (2H, s), 7.06 (1H, t, *J* = 5.4 Hz), 5.08 (2H, d = 5.3 Hz), 3.87 (3H, s), 3.41 (3H, s), 3.21 (3H, s). IR (KBr, cm^{-1}): 3506 (bw), 3277 (m), 2851 (m), 1665 (m), 1658 (m), 1636 (s), 1597 (s), 1526 (m), 1430 (s), 1354 (m), 1231 (s). UV-vis (solid, λ_{max}) 398 nm.

(H44´Bipyridine)$^+$(HL)$^-$: Isolated yield: 69 %. ^{1}HNMR (600 MHz, DMSO, ppm) :12.97 (2H, bs), 8.73 (4H, d, *J* = 6.0 Hz), 8.47 (1H, d, *J* = 9.2 Hz), 8.34-8.24 (5H, m), 8.17 (1H, s), 8.12 – 8.06 (2H, m), 7.84 (4H, dd, *J* = 4.5, 1.6 Hz), 7.70 (1H, s), 7.47 (2H, s), 7.05 (1H, t, *J* = 5.4 Hz), 5.08 (2H, d, *J* = 5.4 Hz). IR (KBr, cm^{-1}) 3473 (w), 3361 (m), 3044 (w), 1699 (s), 1587 (s), 1527 (s), 1461 (s), 1407 (s), 1272 (m), 1208 (s), 840 (s), 795 (s). UV-vis (solid, λ_{max}) 328 nm, 420 nm.

H_2L·0.5Phen: Isolated yield: 68 %. ^{1}H NMR (600 MHz, DMSO) 12.94 (bs, 2H), 8.46 (1H, d, *J* = 9.2 Hz), 8.32 (2H, dd, *J* = 14.3, 7.7 Hz), 8.28 (5H, m), 8.16 (1H, d, *J* = 1.6 Hz), 8.12 – 8.05 (2H,m), 7.98 (2H dd, *J* = 6.7, 3.4 Hz), 7.70 (1H, s), 7.47 (2H, s), 7.05 (1H t, *J* = 5.3 Hz), 5.07 (2H, d, *J* = 5.4 Hz). IR (KBr): 3429 (w), 3130 (w, br), 1706 (s), 1695 (m), 1669 (m), 1608 (s), 1510 (s), 1467 (m), 1417 (w), 1366 (m), 1291 (m), 1182 (s), 1136 (s). UV-vis (solid, λ_{max}) 390-437 (br) nm.

H_2L·PTDA: Isolated yield: 61 %. ^{1}HNMR [(600 MHz, DMSO, ppm): 12.97 (2H, bs), 8.47 (1H, d, *J* = 9.2), 8.34 – 8.23 (5 H, m), 8.16 (1H, s), 8.13 – 8.04 (2H, m), 7.95 (2H, s), 7.70 (1H, s), 7.58-7.39 (5H, m), 7.04 (1H, t, J = 5.5Hz), 6.77 (4H, s), 5.07 (2H, d, J = 5.4). IR (KBr, cm^{-1}) 3437 (m), 3317 (m), 3178 (m, br), 1693 (s), 1620 (s), 1582 (s), 1529 (s), 1493 (m), 1391 (s), 1248 (s). UV-vis (solid, λ_{max}) 307 nm, 390 nm.

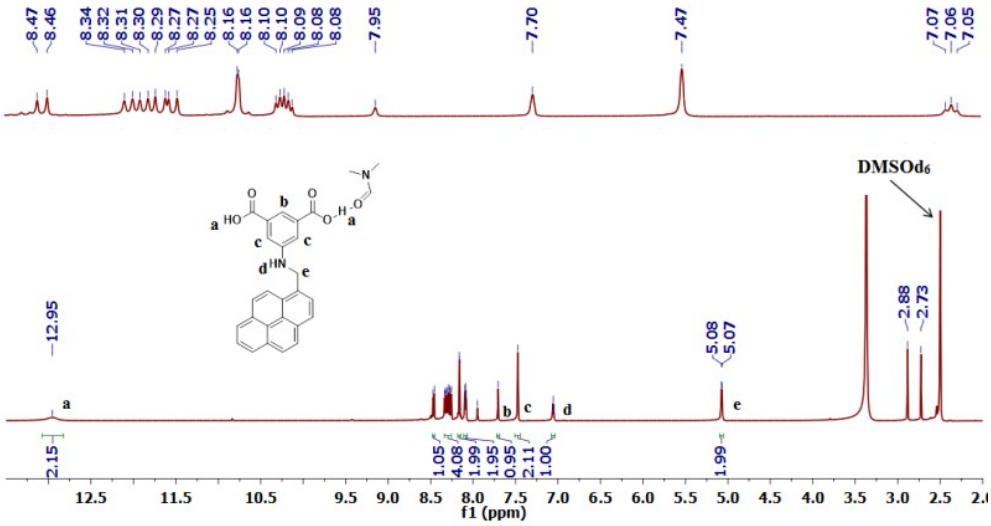

Figure 1S: ^{1}HNMR (400 MHz, DMSO-d$_6$) spectra of **H_2L·DMF**.

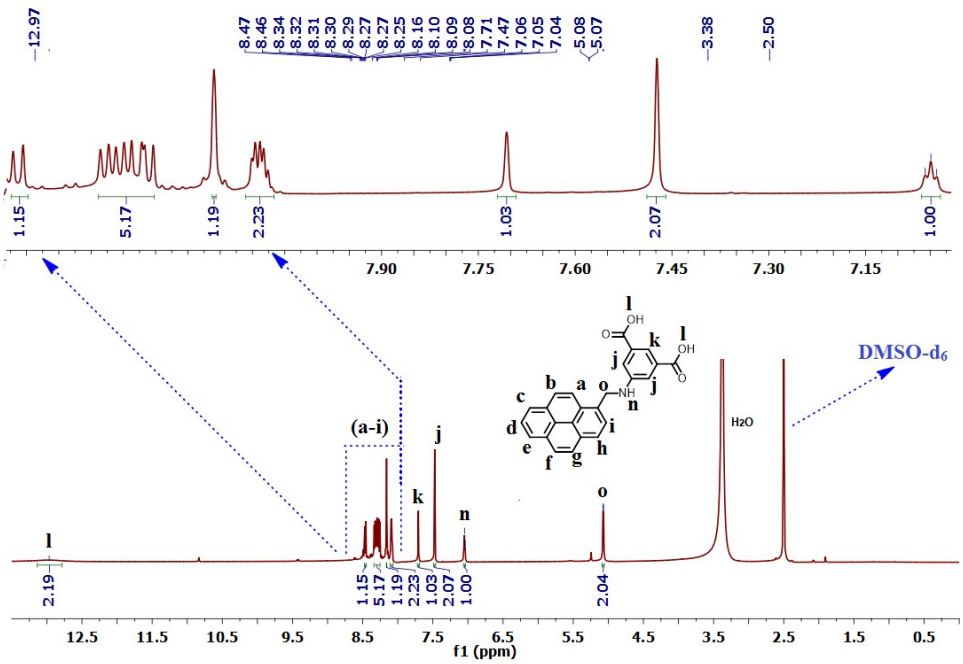

Figure 2S: ^{1}HNMR (400 MHz, DMSO-d_6) spectra of $\mathbf{H_2L}$.

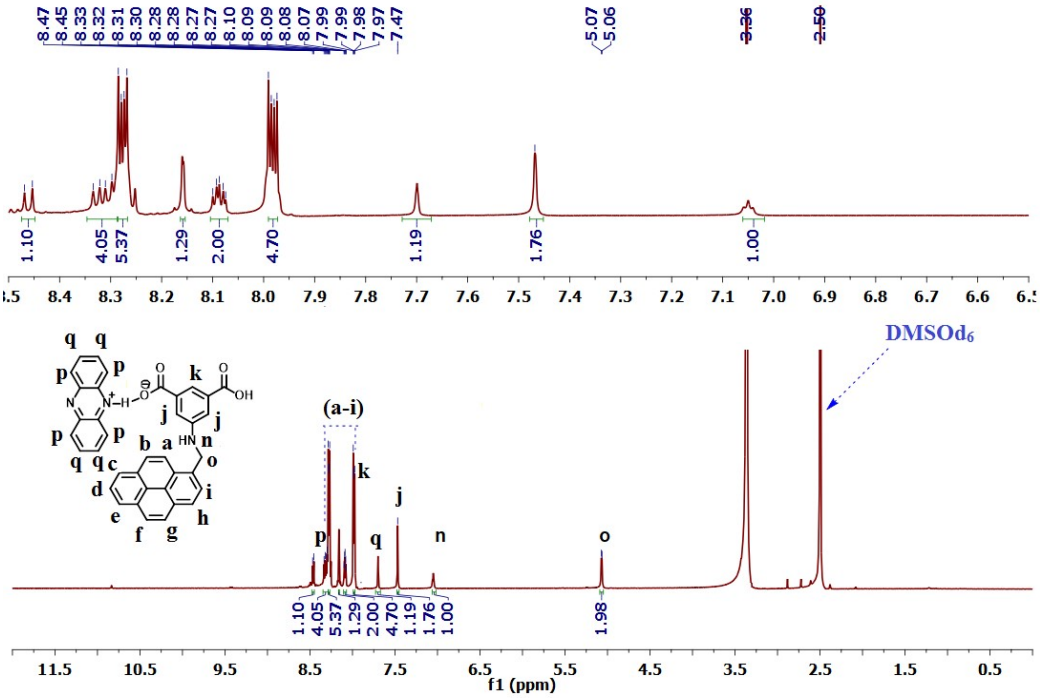

Figure 3S: ^{1}HNMR (600 MHz, DMSO-d_6) $\mathbf{H_2L{\cdot}0.5Phen}$

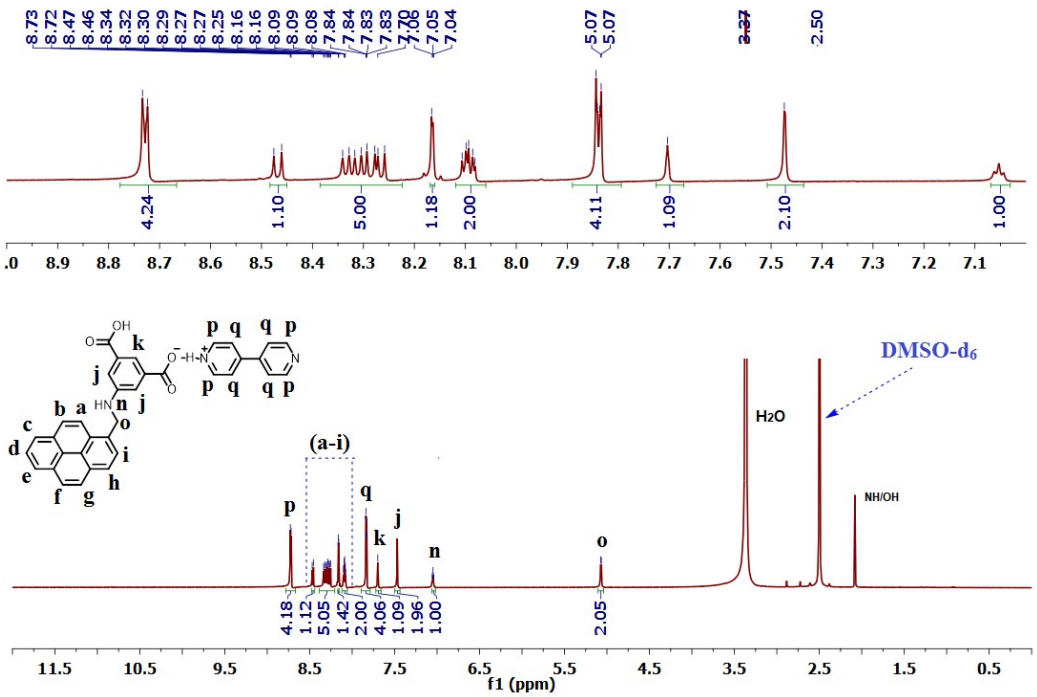

Figure 4S: ^{1}HNMR (600 MHz, DMSO-d_6) spectra of **(H44´Bipyridine)$^{+}$(HL)$^{-}$**.

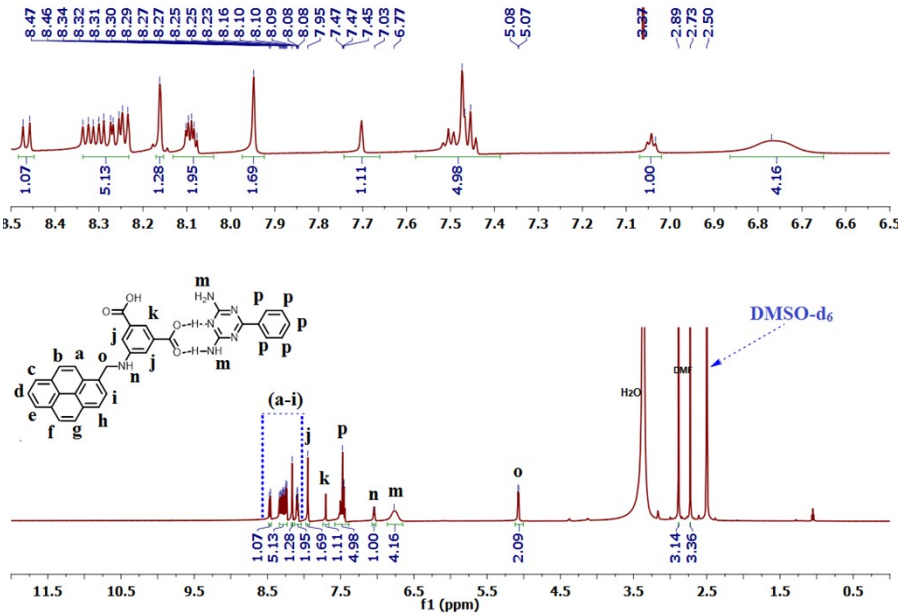

Figure 5S: ^{1}HNMR (400 MHz, DMSO-d_6) spectra of **H_2L·PTDA.**

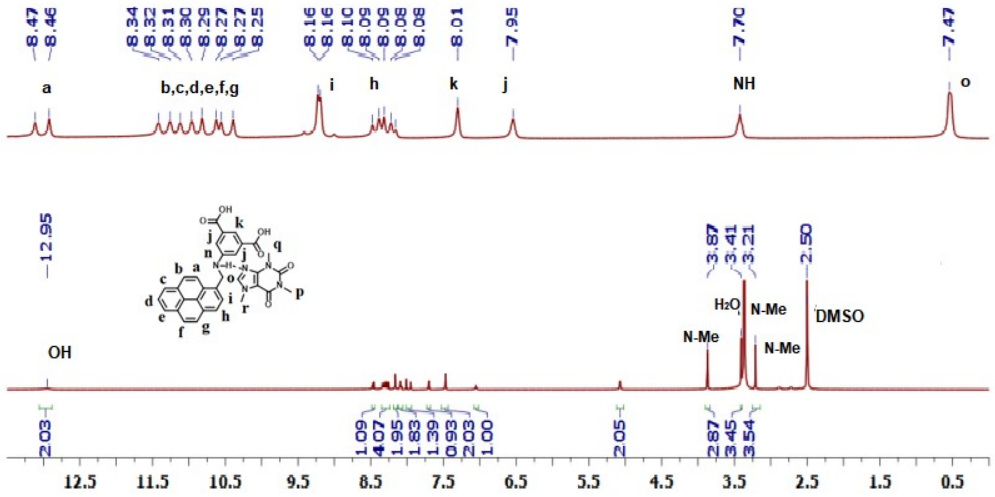

Figure 6S: ^{1}HNMR (400 MHz, DMSO-d_6) spectra of **H_2L·Caffeine·3H_2O**

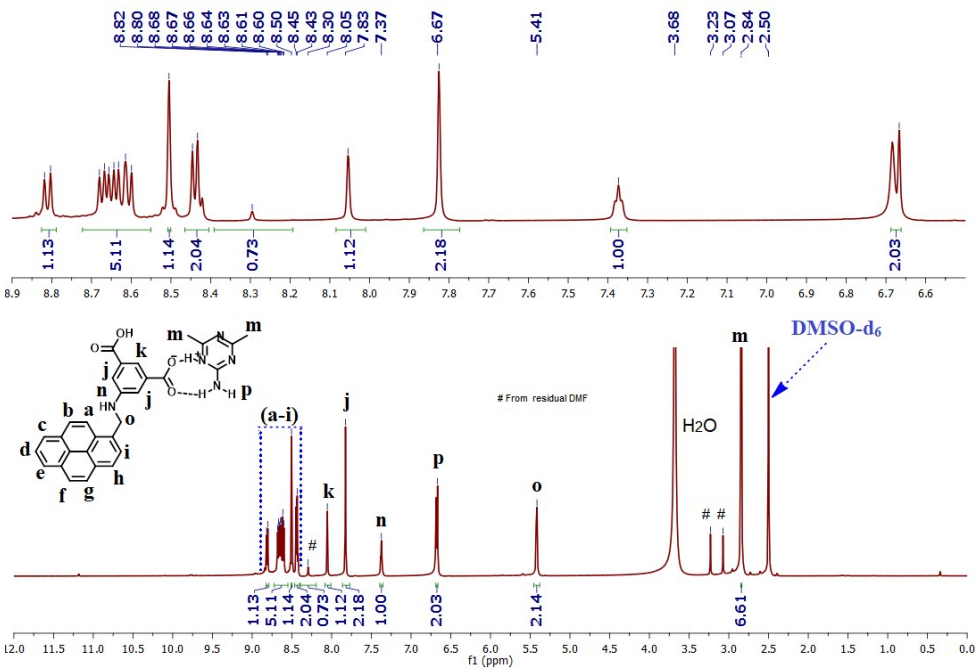

Figure 7S: ^{1}HNMR (400 MHz, DMSO-d_6) spectra of **H_2L·DMPA**.

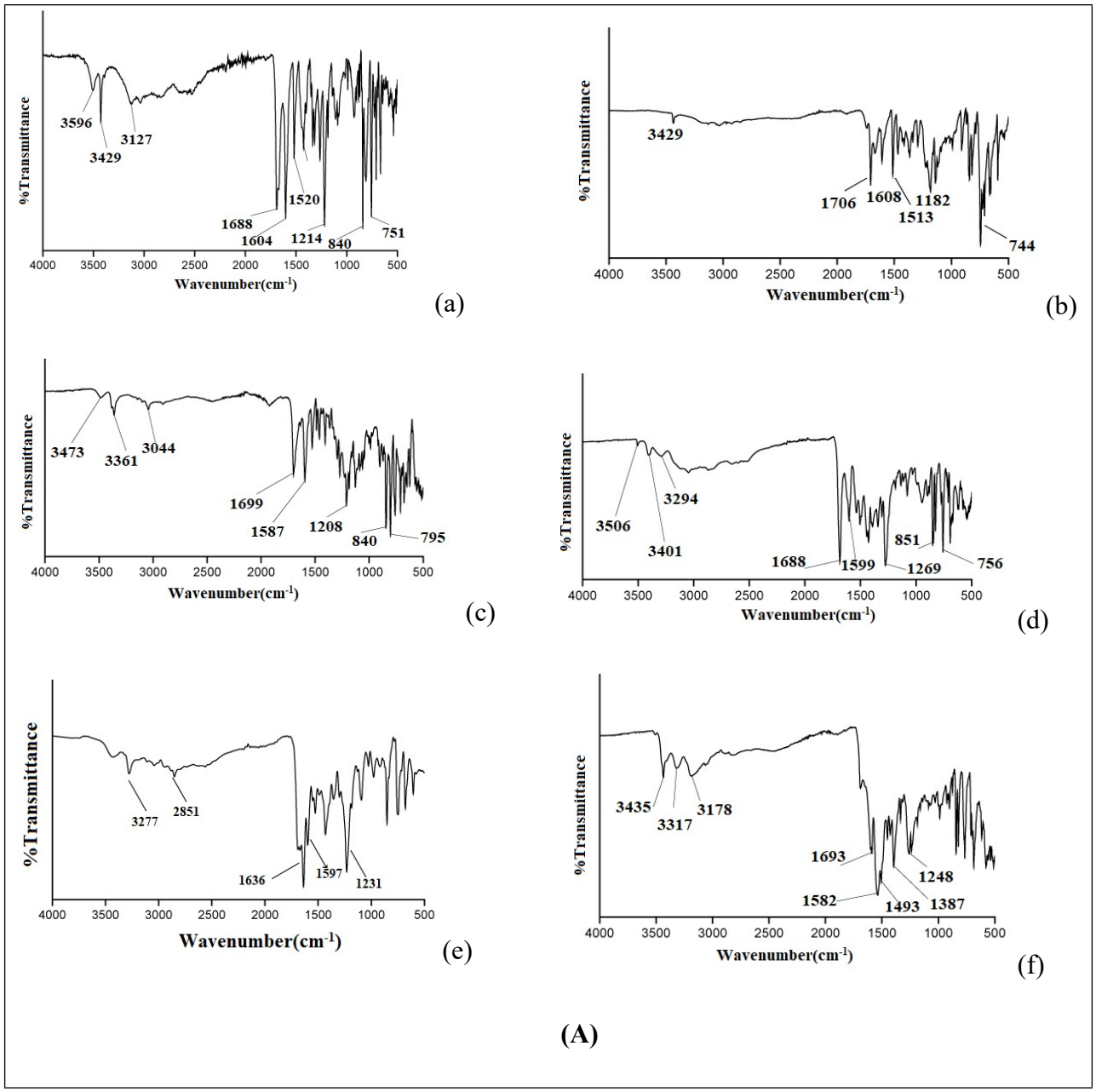
%Transmittance
Wavenumber(cm-1)
3596
3429
3127
1688
1604
1520
1214
840
751
(a)
3429
1706
1608
1182
1513
744
(b)
3473
3361
3044
1699
1587
1208
840
795
(c)
3506
3401
3294
1688
1599
1269
851
756
(d)
3277
2851
1636
1597
1231
(e)
3435
3317
3178
1693
1582
1493
1387
1248
(f)

(A)

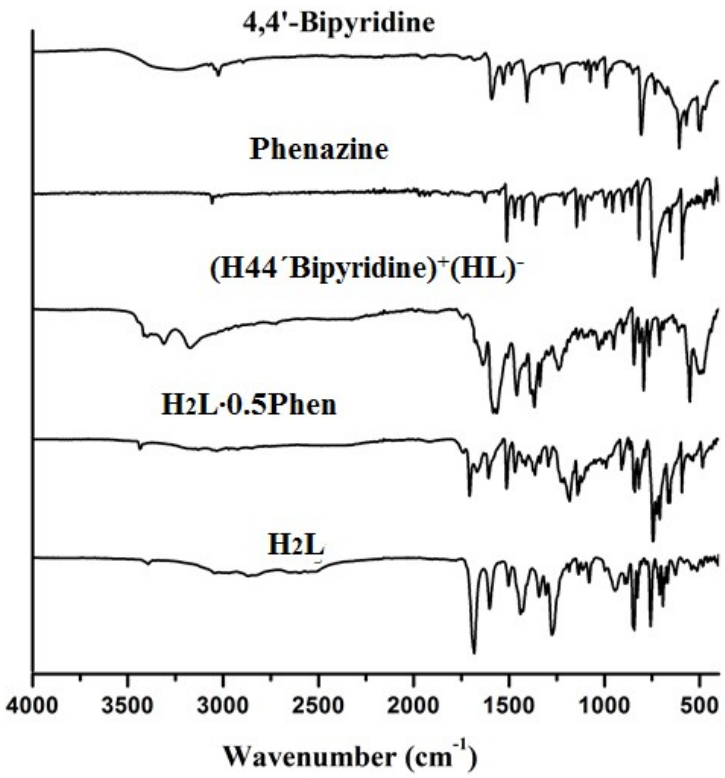

(B)

Figure 8S: (A) IR spectra of (a) **H_2L·DMF**, (b) **H_2L·0.5Phen**, (c) **(H44´Bipyridine)$^+$(HL)$^-$**, (d) **H_2L·DMPA**, (e) **H_2L·Caffeine·3H_2O** and (f) **H_2L·PTDA.** (B) Comparisons of IR spectra of **H_2L·0.5Phen** and **(H44´Bipyridine)$^+$(HL)$^-$** with parent components.

Table 1S: Selected lists of peaks of IR with assignments of the solvates, cocrystals and salt

Compound /Solvate/salt	IR-stretching (cm^{-1}, assignment)
H_2L·DMF	3502 (ν_{O-H})
	3425 (ν_{N-H})
	3102 (νC-H)
	2500-2800 ($\nu_{acid-aldehydic\ synthon}$)
	1668 ($\nu_{C=O,\ DMF}$)
	1658 ($\nu_{C=O,\ carboxylic\ acid}$)
	1601 ($\nu_{C=C}$)
H_2L·PTDA	3437 (ν_{N-H})
	3178 (ν_{C-H})
	1693 ($\nu_{C=O}$)
	1620 ($\nu_{C=C}$)
H_2L·0.5Phen	3429 (ν_{N-H})
	3130 (ν_{C-H})
	1706 ($\nu_{O-H\ overtone}$)
	1695 ($\nu_{C=O}$)
	1669 ($\nu_{C=O}$)

	1608 ($\nu_{C=c}$)
H_2L·DMPA	3506 (ν_{O-H})
	3401 (ν_{N-H})
	3294 (ν_{C-H})
	1883 ((ν_{amide})
	1688 ($\nu_{C=O}$)
	1664 ($\nu_{C=O}$)
H_2L·Caffeine·3H_2O	3506 (ν_{0-H})
	3277 (ν_{N-H})
	2851 ($\nu_{acid-acid\ synthon}$)
	1665 ($\nu_{c=o}$)
	1658 ($\nu_{c=o}$)
	1231 ($\nu_{C-H\ in\ plane\ deformation}$)
(H44´Bipyridine)$^+$(HL)$^-$	3473 ((ν_{N+-H})
	3361 (ν_{o-H})
	3044 ((ν_{c-H})
	1699 ($\nu_{c=o}$)
	1587 (($\nu_{c=C}$)
	1527 ($\nu_{ring\ bipyridine}$)

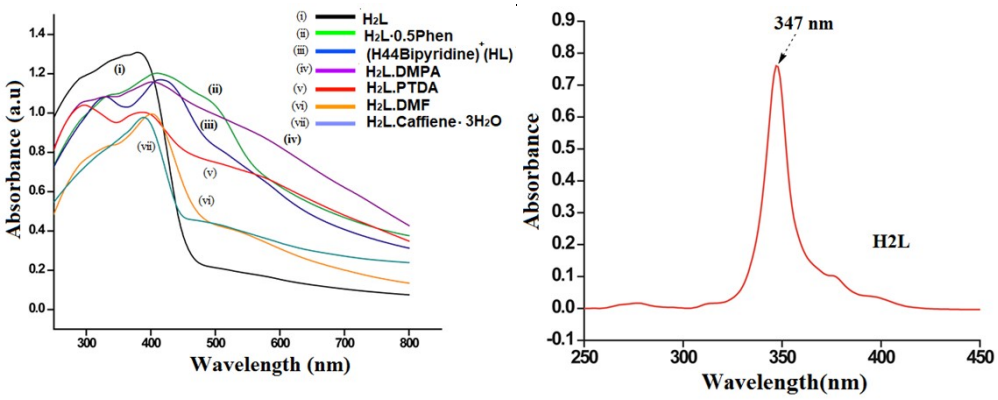

(a) (b)

Figure **9S:** (a) UV-vis spectra of the solid samples of **H_2L** and co-crystals, (b) UV-visible spectrum of **H_2L** in DMSO (10^{-3} M).

Table 2S: Hydrogen bond parameters of solvate, co-crystals and salt of **H_2L**

Compound	D-H⋯A	d_{D-H} (Å)	$d_{H\cdots A}$ (Å)	$d_{D\cdots A}$ (Å)	∠D-H⋯A (º)
H_2L·DMF	O(1)-H(1A)⋯O(5) [-1+x,y,z]	0.82	1.77	2.584(4)	176
	O(4)-H(4)⋯O(2) [x,-1+y,z]	0.82	1.81	2.619(3)	167
	C(26)-H(26)⋯O(2) [1+x,y,z]	0.93	2.44	3.142(4)	133
H_2L·DMPA	O(1)-H(1A)⋯N(3) [x,-1+y,1+z]	0.89(3)	1.83(3)	2.708(3)	170(3)
	N(2)-H(2A)⋯O(3) [x,y,-1+z]	0.91(3)	1.94(3)	2.834(3)	168(2)
	N(2)-H(2B)⋯O(2) [x,1+y,-1+z]	0.89(3)	1.98(3)	2.844(3)	164(2)

	O(4)-H(4)···N(4) [x,y,1+z]	0.99(4)	1.68(4)	2.668(3)	173(3)
H_2L·Caffeine·$3H_2O$	N(1)-H(1)···N(4) [-1+x,y,z]	0.85(8)	2.24(8)	3.076(11)	169(9)
	O(1)-H(1A)···O(2) [-1-x,1-y,1-z]	0.82	1.83	2.652(10)	175
	O(3)-H(3)···O(1) [1+x,y,z]	0.82	2.60	3.316(11)	147
	O(7)-H(7A)···O(3) [1-x,1-y,1-z]	0.85	1.80	2.598(12)	156
	O(7)-H(7B)···O(8) [x,y,z]	0.85	1.94	2.785(19)	177
	C(16)-H(16)···O(2) [1+x,y,z]	0.93	2.50	3.356(13)	153
	C(28)-H(28B)···O(4) [1-x,1-y,1-z]	0.96	2.49	3.423(14)	163
	C(33)-H(33A)···O(5) [x,y,z]	0.96	2.50	3.182(15)	128
(H44´Bipyridine)$^+$(HL)$^-$	N(1)-H(1)···O(3) [3-x,1-y,1-z]	0.99(8)	2.13(7)	3.113(8)	174(7)
	O(1)-H(1A)···O(4) [3-x,1-y,-z]	0.93(6)	1.79(6)	2.698(7)	163(6)
	N(3)-H(3A)···O(4) [3-x,1-y,1-z]	0.88(6)	1.70(5)	2.570(8)	176(10)
	C(7)-H(7)···O(1) [3-x,1-y,-z]	0.93	2.38	3.232(8)	152
	C(33)-H(33)···O(2) [x,y,1+z]	0.93	2.34	3.223(9)	159
H_2L·0.5Phen	O(1)-H(1A)···N(2) [1-x,1-y,-z]	0.82	1.99	2.794(3)	165
	O(4)-H(4)···O(2) [1+x,y,z]	0.82	1.91	2.696(4)	161
	C(30)-H(30)···O(2) [1-x,1-y,-z]	0.93	2.41	3.308(4)	162
H_2L·PTDA					
	O(2)-H(2)···N(4) [-x,-y,1-z]	0.82	1.99	2.803(3)	171
	N(2)-H(2A)···O(4) [1+x,y,-1+z]	0.86	2.26	3.039(3)	151
	N(2)-H(2B)···O(4) [1-x,1-y,1-z]	0.86	2.05	2.871(3)	159
	O(3)-H(3A)···N(3) [1-x,1-y,1-z]	0.82	1.95	2.758(3)	170
	N(5)-H(5A)···O(1) [-x,-y,1-z]	0.90(3)	1.96(3)	2.857(4)	175(3)
	N(5)-H(5B)···O(1) [1+x,y,-1+z]	0.91(3)	2.10(3)	3.000(4)	168(3)

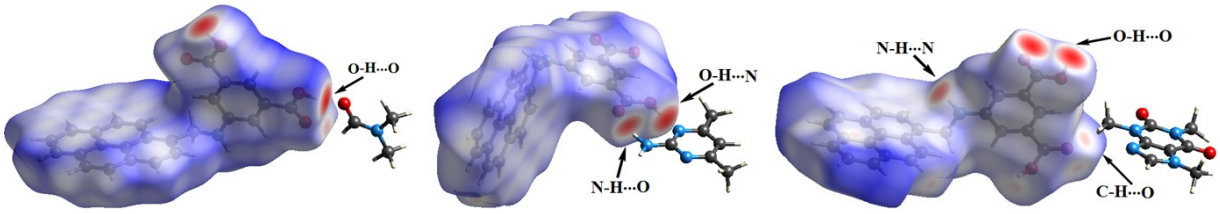

(a) (b) (c)

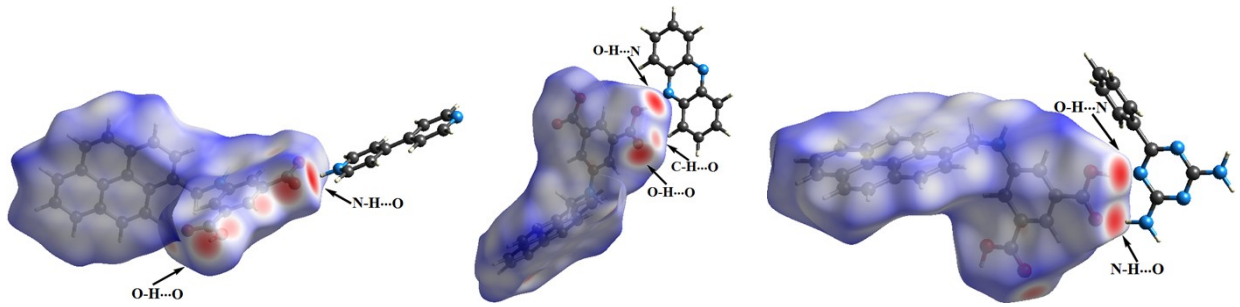

(d) (e) (f)

Figure 10S: Hirshfeld surfaces of (a) **H_2L·DMF**; (b) **H_2L·DMPA**; (c) **H_2L·Caffeine·3H_2O**; (d) **(H44´Bipyridine)$^+$(HL)$^-$**; (e) **H_2L·0.5Phen** and (f) **H_2L·PTDA.**

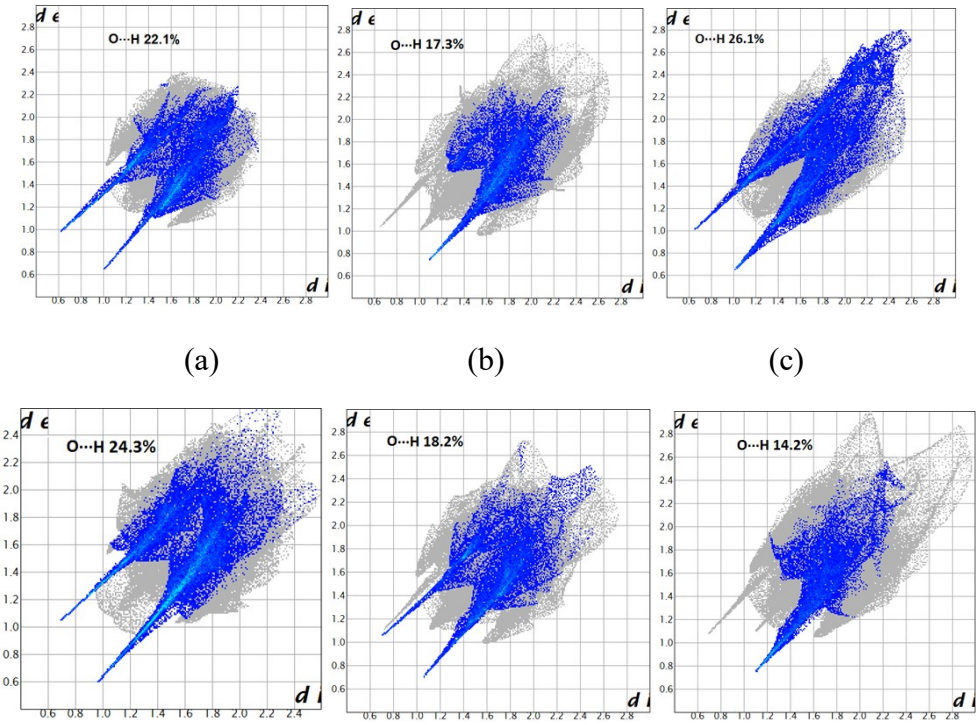

(a) (b) (c)

(d) (e) (f)

Figure 11S: Fingerprint plots for (a) **H_2L·DMF**; (b) **H_2L·DMPA**; (c) **H_2L·Caffeine·3H_2O**; (d) **(H44´Bipyridine)$^+$(HL)$^-$**; (e) **H_2L·0.5Phen** and (f) **H_2L· PTDA** (O···H interactions highlighted in blue color)

Table 3S: Contributions from different interactions calculated from Hirshfeld surface analysis by using the CIF files of the **H_2L** solvate, cocrystals and salt

Bond	**H_2L·DMF**	**H_2L· DMPA**	**H_2L· Caffeine ·H_2O**	**(H44´Bipyridine) $^+$(HL)$^-$**	**H_2L·0.5Phen**	**H_2L· PTDA**
O···O	0.5	0.1	1.1	0.7	0.8	0.1
N···O	0.4	0.3	0.0	0.1	0.0	0.7
C···O	1.0	0.8	3.3	0.9	1.5	2.2
H···O	22.1	17.3	26.1	24.3	18.2	14.2
C···N	0.2	1.0	3.5	0.4	1.2	0.8
N···H	0.2	4.2	2.2	1.3	1.9	5.4
C···H	26.1	25.3	17.8	25.8	26.2	34.9
C···C	10.2	7.8	6.5	8.4	11.6	4.2
H···H	39.3	43.2	39.4	38.2	38.6	37.4

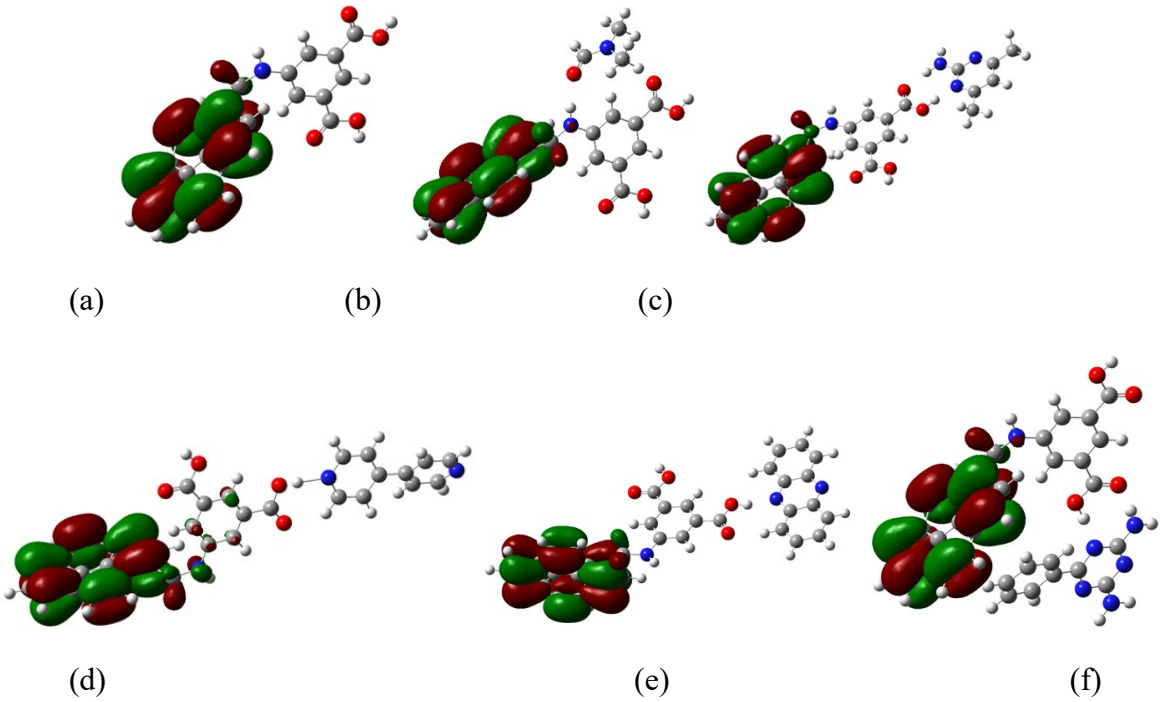

Figure 12S: HOMO of (a) **H_2L**; (b) **H_2L.DMF**; (c) **H_2L.DMPA**; (d) **(H44´Bipyridine)$^+$(HL)$^-$**; (e) **H_2L·0.5Phen** and (f) **H_2L·PTDA**.

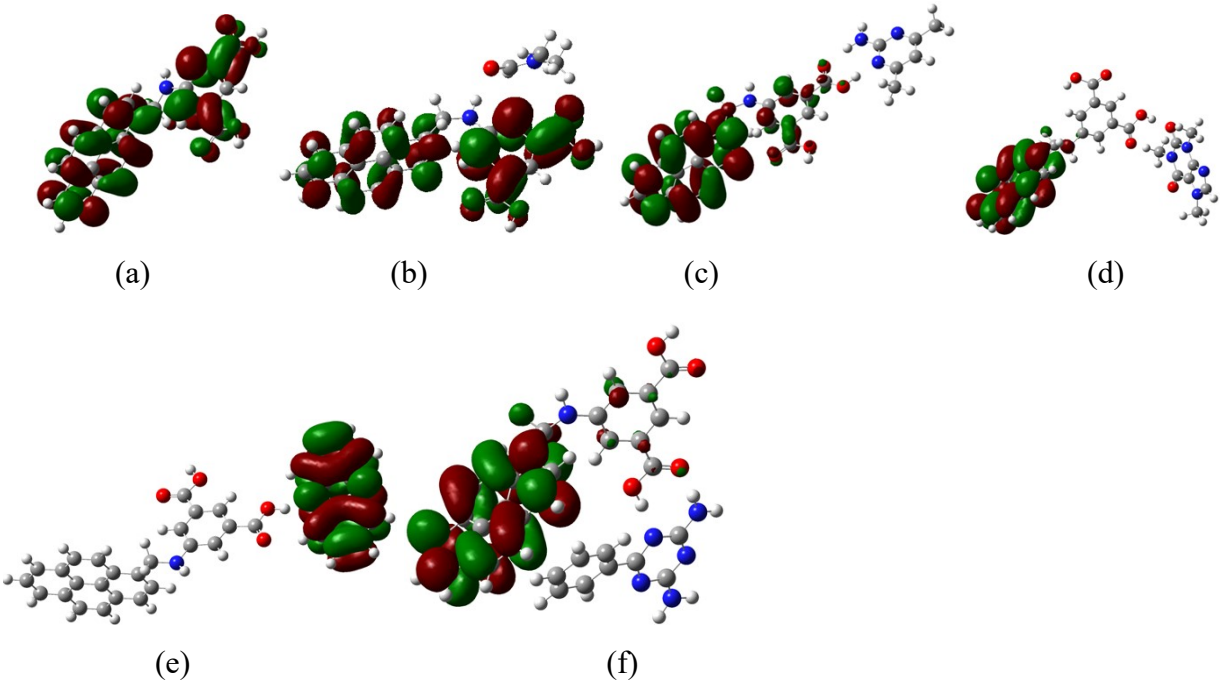

Figure 13S: LUMO of (a) **H_2L**; (b) **H_2L·DMF;** (c) **H_2L·DMPA**; (d) **(H44´Bipyridine)$^+$(HL)$^-$**; (e) **H_2L·0.5Phen** and (f) **H_2L·PTDA**.

Table 4S: HOMO-LUMO energy obtained from DFT calculation for **H_2L** and its solvate, co-crystals and salt

Compounds	HOMO (eV)	LUMO (eV)	Energy difference = HOMO-LUMO (eV)
H_2L	-5.3304	-1.6272	3.7032
H_2L·DMF	-5.1543	-1.4797	3.6746
H_2L·DMPA	-5.2700	-1.5396	3.7304
(H44´Bipyridine)$^+$(HL)$^-$	-5.2790	-1.9994	3.2796
H_2L·0.5Phen	-5.2621	-2.7298	2.5323
H_2L·PTDA	-5.4218	-1.6892	3.7326

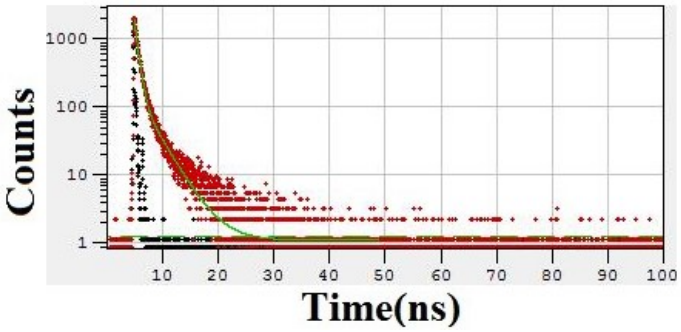

Figure 14S: Time resolved fluorescence emission of solid sample of **H_2L** (λ_{ex} = 375 nm, λ_{em} = 460 nm).

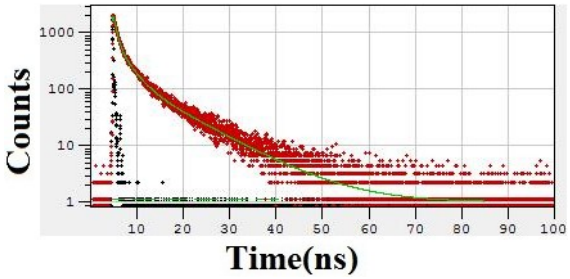

Figure 15S: Time resolved fluorescence emission of solid sample of **H_2L·DMF** (λ_{ex} = 375nm, λ_{em} = 470 nm).

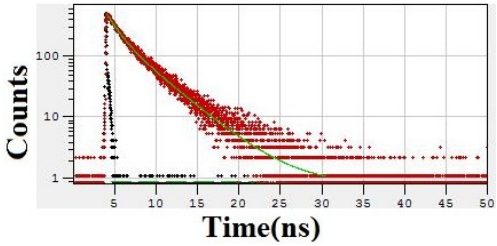

Figure 16S: Time resolved fluorescence emission of solid sample of **H_2L·Caffeine·3H_2O** (λ_{ex} = 375 nm, λ_{em} = 415 nm).

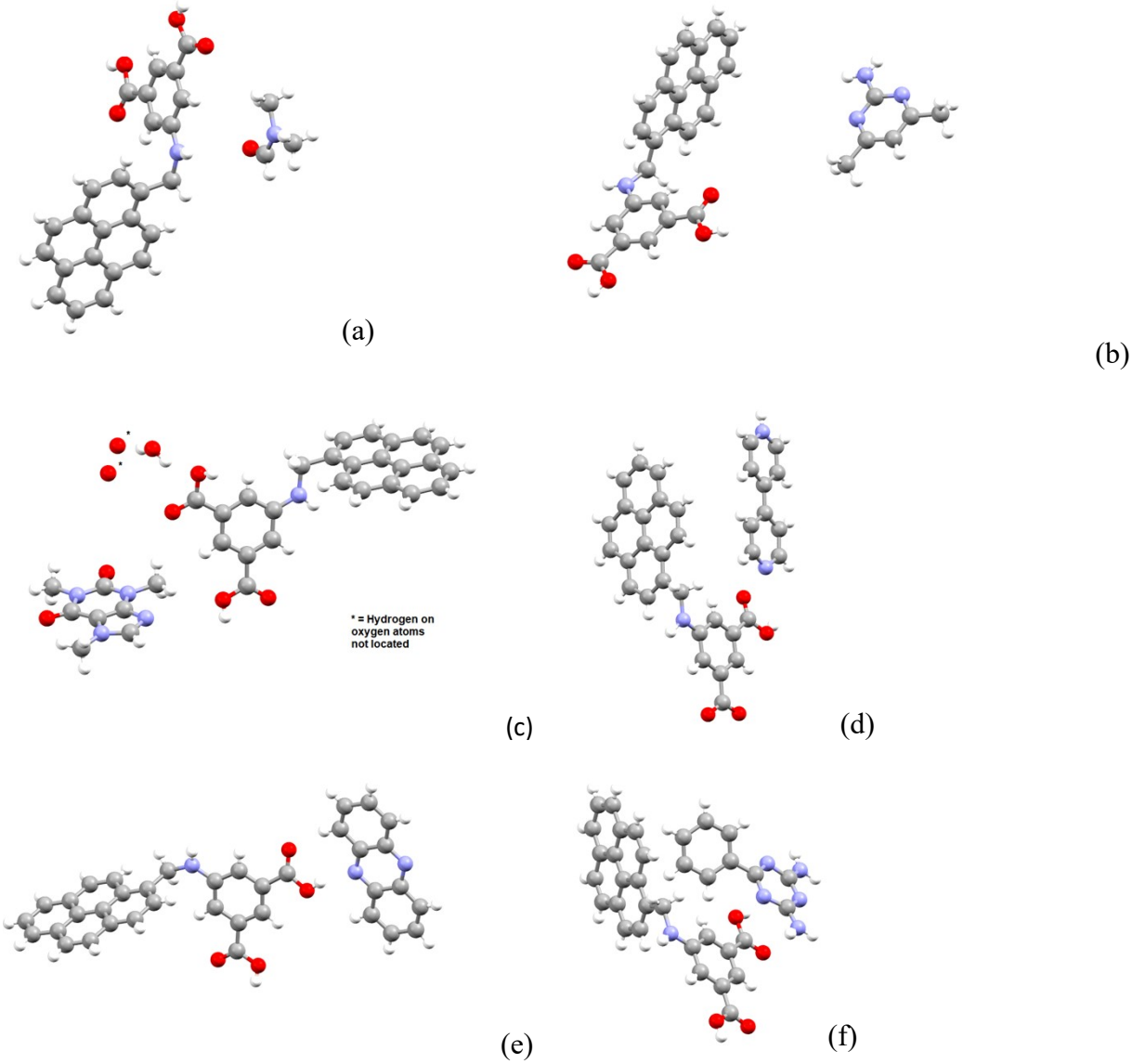

Figure 17S: The crystal structures drawn using POV-Ray of (a) **H_2L.DMF**; (b) **H_2L.DMPA**; (c) **H_2L·Caffeine·3H_2O**; (d) **(H44´Bipyridine)$^+$(HL)$^-$**; (e) **H_2L·0.5Phen** and (f) **H_2L·PTDA (Color code : Red = Oxygen, Blue = Nitrogen, white = Hydrogen, cyan = Carbon atoms)**.

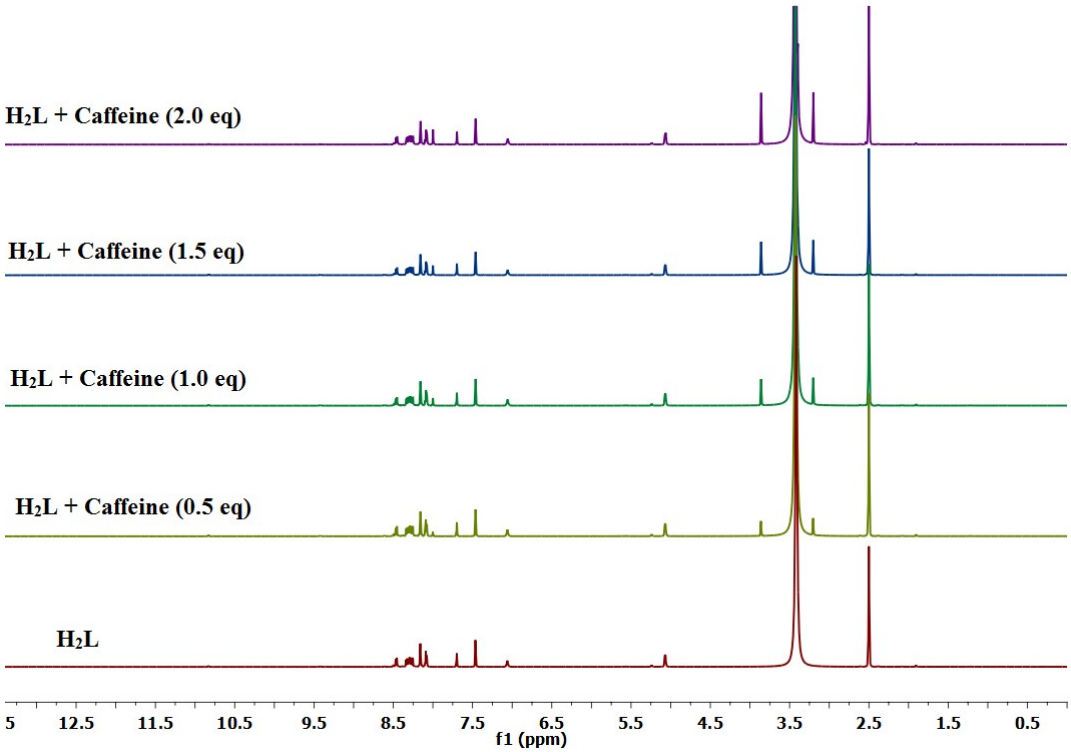

Figure 18S: ^{1}HNMR (600MHz, DMSO-d_6) titration of **H_2L** with different amounts of caffeine.

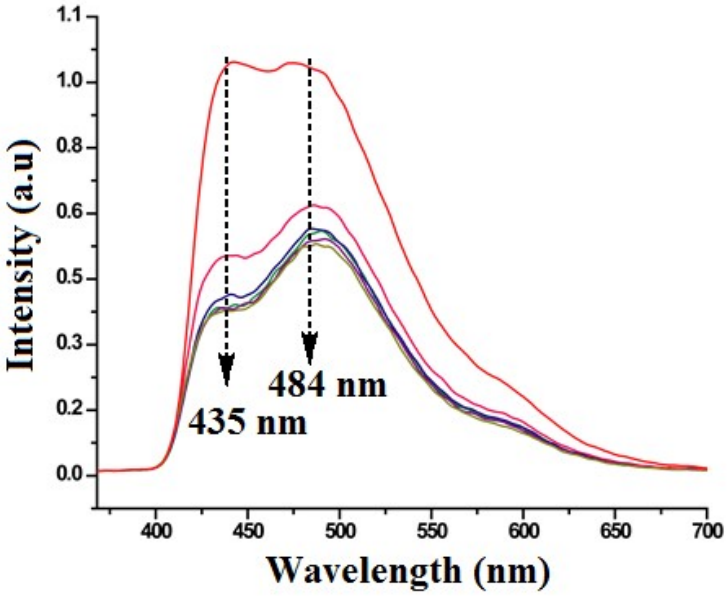

Figure 19S: (a) Decrease in the fluorescence emission intensities of **H_2L** in DMSO (10^{-3} M, 3 mL) upon addition of different aliquots of caffeine solution in DMSO (10^{-3} M, 20µL in each aliquot).

Table 5S: Fluorescence life-time decay data for the **H_2L** and its solvate, co-crystals and salt

H_2L or Cocrystal	Exponential component	f_i (%)	τ_i (ns)	χ^2
H_2L	1	82.033	0.560	1.000
	2	17.967	3.078	
H_2L·DMF	1	24.107	0.526	0.999
	2	36.518	2.494	
	3	39.375	9.688	
H2L·Caffeine·3H_2O	1	30.078	1.330	1.134
	2	69.922	3.911	

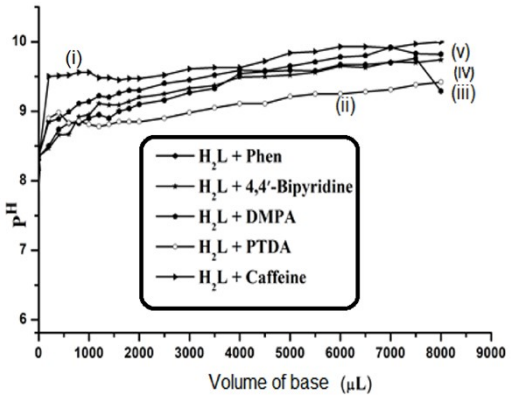

Figure 20S **:** The pH titrations of the **H_2L** (2 ml of 1mM in DMF) with (i) Caffeine, (ii) PTDA, (iii) Phenazine, (iv) 4,4′-Bipyridine, (v) DMPA, (vi) (1mM of respective compound in DMF).

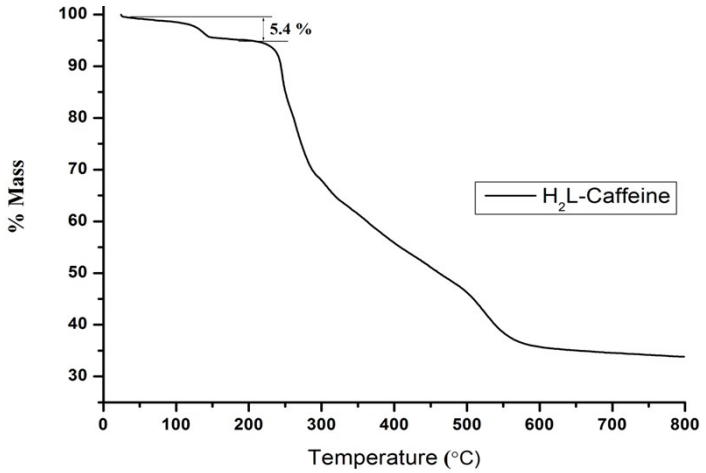

Figure 21S: The thermogram of **H_2L·Caffeine·3H_2O** (heating rate 10˚C/min)

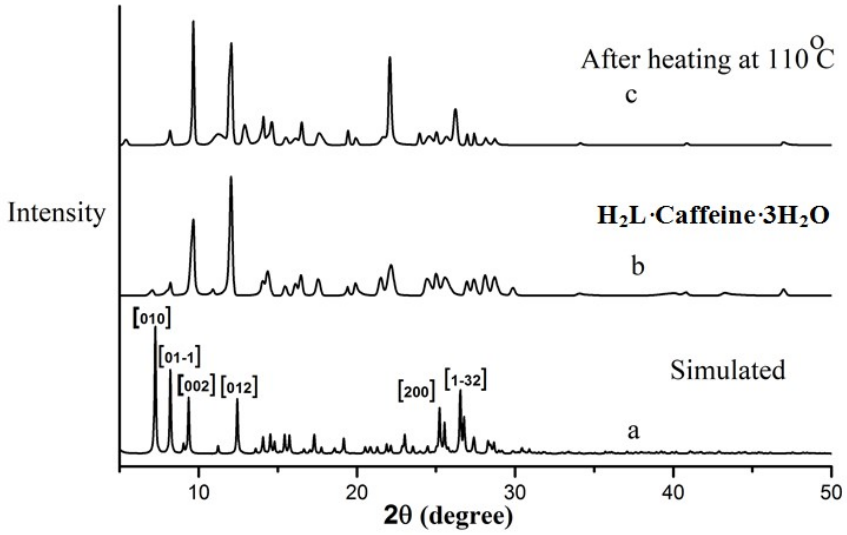

Figure 22S: The powder X-ray diffraction patterns of the **H_2L·Caffeine·$3H_2O$**, (a) simulate from the crystallographic information file and experimentally determined from powdered sample (a) in the hydrated form, (c) after heating the sample at 110˚C for 2 hrs PXRD was recorded at room temperature.